Covalent bonds against magnetism in transition metal compounds

Sergey V. Streltsov[a,b,1] and Daniel I. Khomskii[c]

[a]Optics of Metals Laboratory, Institute of Metal Physics, 620990 Yekaterinburg, Russia; [b]Department of Theoretical Physics and Applied Mathematics, Ural Federal University, 620002 Yekaterinburg, Russia; and [c]II. Physikalisches Institut, Universität zu Köln, D-50937 Köln, Germany

Edited by Robert Joseph Cava, Princeton University, Princeton, NJ, and approved July 15, 2016 (received for review April 22, 2016)

Magnetism in transition metal compounds is usually considered starting from a description of isolated ions, as exact as possible, and treating their (exchange) interaction at a later stage. We show that this standard approach may break down in many cases, especially in 4*d* and 5*d* compounds. We argue that there is an important intersite effect—an orbital-selective formation of covalent metal–metal bonds that leads to an "exclusion" of corresponding electrons from the magnetic subsystem, and thus strongly affects magnetic properties of the system. This effect is especially prominent for noninteger electron number, when it results in suppression of the famous double exchange, the main mechanism of ferromagnetism in transition metal compounds. We study this mechanism analytically and numerically and show that it explains magnetic properties of not only several 4*d*–5*d* materials, including $Nb_2O_2F_3$ and $Ba_5AlIr_2O_{11}$, but can also be operative in 3*d* transition metal oxides, e.g., in CrO_2 under pressure. We also discuss the role of spin–orbit coupling on the competition between covalency and magnetism. Our results demonstrate that strong intersite coupling may invalidate the standard single-site starting point for considering magnetism, and can lead to a qualitatively new behavior.

double exchange | magnetism | transition metal compounds

Transition metal (TM) compounds present one of the main playgrounds in a large field of magnetism (1–3). Usually, when considering magnetic properties of these systems, one starts from the, as exact as possible, treatment of isolated TM ions or such ions in the surrounding of ligands, e.g., TMO_6 octahedra. A typical situation for a moderately strong crystal field is the one in which *d* electrons obey the Hund's rule, forming a state with the maximal spin. For a stronger crystal field low-spin states are also possible, but also in this case electrons in degenerate subshells, e.g., t_{2g} electrons, first form a state with maximal possible spin. Then, these large total spins interact by exchange coupling with the neighboring TM ions. This interaction, a superexchange for integer electron occupation (4), or a double exchange for partially filled *d* levels (5), is then treated using this starting point with this total spin of isolated ions, taking into account the hopping between sites (leading in effect to magnetic interaction) as a weak perturbation, which does not break the magnetic state of an ion.

For heavier elements, such as 4*d* or 5*d* TM, one should also take into account the relativistic spin–orbit (SO) coupling, which couples the total spin *S* as dictated by the Hund's rule, with the (effective) orbital moment *L*. In any case, it is usually assumed that the "building blocks" for further consideration of the magnetic interactions are such isolated TM ions with the corresponding quantum numbers.

However, especially when we go to heavier TM ions, such as 4*d* and 5*d*, also the spatial extent of the corresponding *d* orbitals increases strongly, and with it the effective *d*–*d* hopping, *t* (2). One can anticipate a possibility for this hopping to become comparable with or even exceed the intra-atomic interactions, such as the Hund's coupling, J_H, and spin–orbit coupling λ. In such a case the standard approach described above may break down and one has to include intersite effects from the very beginning. We claim that this indeed happens in many 4*d* and 5*d* systems with appropriate geometries. The resulting effect is that, for example, in a TM dimer with several *d* electrons per ion, some electrons, namely those occupying the orbitals with the strongest overlap, form intersite covalent bonds, i.e., the singlet molecular orbitals (MO). In this case such electrons become essentially nonmagnetic and "drop out of the game," so that only *d* electrons in orbitals without such a strong overlap may be treated as localized, contributing to localized moments and to eventual magnetic ordering. The result would be that the effective magnetic moment of a TM ion in such situation would become much smaller than the nominal moment corresponding to the formal valence of an ion. Below we demonstrate that this effect is indeed realized in many TM compounds, especially those of 4*d* and 5*d* elements. Besides reducing the magnetic moment of an ion, this mechanism can suppress the well-known double exchange (DE) mechanism of (ferro)magnetic ordering—the main mechanism of ferromagnetism in systems with a fractional occupation of the *d* levels.

Before presenting the main results, let us emphasize that the interplay between the formation of covalent bonds, spin–orbit coupling, and intra-atomic exchange interaction discussed in the present paper is very important for intensively studied nowadays 4*d* and 5*d* transition metal oxides such as $\alpha-RuCl_3$ (6, 7), Li_2RuO_3 (8, 9), $LiZn_2Mo_3O_8$ (10, 11), and Na_2IrO_3 (12–14). Competition of these interactions results in highly unusual physical properties in these systems: Kitaev spin liquid, valence–bond condensation, and different topological effects.

Qualitative Considerations

We start by simple qualitative arguments, considering a two-site problem with, for example, three electrons per dimer, occupying two types of orbitals: orbital *c* (the corresponding creation and

Significance

A mechanism by which orbital degrees of freedom can strongly affect magnetic properties of systems with correlated electrons is proposed. Using analytical treatment and numerical simulations, both in general and for some particular substances, we show that the formation of covalent bonds on part of the orbitals may strongly reduce magnetic moments and explain magnetic properties of different 4*d* and 5*d* transition metal oxides. In particular, orbital-selective effects may result in suppression of double exchange—one of the main mechanisms of ferromagnetism in transition metals and compounds, such as colossal magnetoresistance manganites or CrO_2—the materials used in many devices.

Author contributions: S.V.S. and D.I.K. performed research and wrote the paper.

The authors declare no conflict of interest.

This article is a PNAS Direct Submission.

[1]To whom correspondence should be addressed. Email: streltsov@imp.uran.ru.

This article contains supporting information online at www.pnas.org/lookup/suppl/doi:10.1073/pnas.1606367113/-/DCSupplemental.

annihilation electron operators at the site i with the spin σ are $c^{\dagger}_{i\sigma}$, $c_{i\sigma}$), with intersite hopping t_c, and another orbital, d, with a very weak hopping t_d (which we for simplicity at the beginning put to zero). In reality the c orbitals could be, for example, the strongly overlapping xy orbitals in the situation when the neighboring TMO_6 octahedra share edges, i.e., have two common oxygens, see Fig. 1*A*, or the a_{1g} orbitals in the common face geometry, Fig. 1*B*; the orthogonal orbitals (zx, yz in the first case or e^{π}_g orbitals in the second) would then play a role of localized d orbitals (for a more detailed treatment of these situations see, e.g., refs. 15–17).

In this case we can consider two different limiting states. In the state depicted in Fig. 2*A* we put two electrons into the localized d orbitals, and the remaining electron occupies the "itinerant" c orbital, hopping back and forth from site 1 to site 2, or occupying the bonding state $(c^{\dagger}_{1\uparrow}+c^{\dagger}_{2\uparrow})/\sqrt{2}$. To optimize the Hund's intra-atomic exchange, this "hopping" electron would have its spin parallel to the spins of the localized electrons, and its delocalization stabilizes the state with maximum spin, here $S_{tot}=3/2$. This is, in essence, the double exchange mechanism of ferromagnetism, first proposed by Zener for just such a dimer (5). It is easy to see that the energy of this DE state is

$$E_{DE} = -t_c - J_H. \quad [1]$$

For simplicity we ignore here the contribution of the onsite Coulomb (Hubbard) interaction, see a more complete treatment below. We also treat the Hund's interaction

$$H_{Hund} = -J_H\left(1/2 + 2\vec{S}_1\vec{S}_2\right), \quad [2]$$

in the mean-field approximation, where $\vec{S}_1$ and $\vec{S}_2$ are the total spins on sites 1 and 2.

This DE state is definitely the most favorable state for a strong Hund's interaction. Indeed, in all papers on double exchange (5, 18, 19) one makes such an approximation, most often by simply setting J_H to infinity. This is a reasonable assumption for most 3*d* compounds at ambient conditions, for which $J_H \sim$ 0.7–0.9 eV, usually (much) larger than the effective *d*–*d* hopping (direct, or via ligands), which is typically 0.1–0.3 eV. However, when we go to 4*d*, and especially 5*d* systems, the situation may change drastically: J_H is reduced (20) (to ∼ 0.5–0.6 eV for 4*d* and ∼ 0.5 eV for 5*d* elements; ref. 21); whereas, the spatial extension of *d*-wave

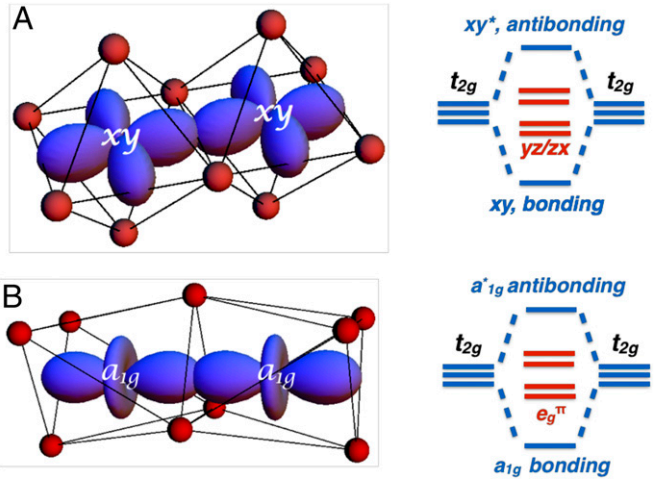

Fig. 1. Orbitals having large overlap (*c* orbitals in our notations) and corresponding level splitting with the formation of bonding and antibonding orbitals for transition metal dimers in different geometries: (*A*) common edge geometry and *xy* orbitals, and (*B*) common face geometry and $a_{1g}-$ orbitals.

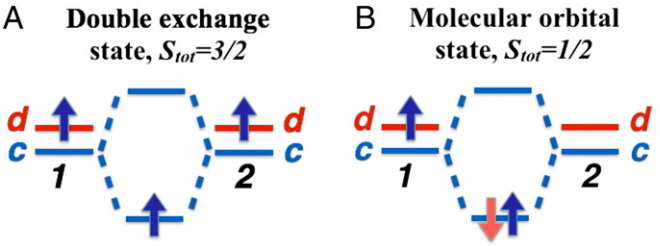

Fig. 2. Two competing electronic configurations with different total spin S_{tot}: (*A*) DE and (*B*) MO states for a dimer with two orbitals (*c* and *d*) per site and three electrons.

function, and the corresponding overlap and *d*–*d* hopping strongly increase, so that t_c can easily be of order of 1.0–1.5 eV, as e.g., in Li_2RuO_3 (8) or $Y_5Mo_2O_{12}$ (22). In this case we can form a different state (illustrated in Fig. 2*B*), redistributing electrons between *d* orbitals: we now put two electrons on the itinerant *c* orbitals, so that they form a singlet state in the bonding orbital of Fig. 2*B* (actually a molecular orbital state):

$$|MO\rangle = \left(c^{\dagger}_{1\uparrow}+c^{\dagger}_{2\uparrow}\right)\left(c^{\dagger}_{1\downarrow}+c^{\dagger}_{2\downarrow}\right)\Big/2, \quad [3]$$

leaving one electron on localized *d* orbitals. In effect, the total spin of this state (we call it for short the MO state) is not 3/2, as for the DE state of Fig. 2*A*, but only $S_{tot}=1/2$. The energy of this state in our simple approximation is

$$E_{MO} = -2t_c - J_H/2. \quad [4]$$

Comparing the energies **[1]** and **[4]**, we see that the MO state with suppressed double exchange and strongly reduced total spin is more favorable if

$$2t_c > J_H. \quad [5]$$

Thus, we observe that in this simplified model the covalent bonding, defined by the hopping t_c (which can include also the hopping via ligands), can suppress the DE.

One can use a more general wave function of MO type, with two electrons in the *c* orbitals with the total $S=0$, and one localized electron with $S=1/2$ in *d* orbitals. For example, if we put *d* electron with spin ↑ at a site 1, we can take generalized MO state in the form

$$\left|\widetilde{MO}\right\rangle = \left(\alpha c^{\dagger}_{1\uparrow}+\beta c^{\dagger}_{2\uparrow}\right)\left(\beta c^{\dagger}_{1\downarrow}+\alpha c^{\dagger}_{2\downarrow}\right)\Big/2, \quad [6]$$

with the variational parameters α, β such that $\alpha>\beta$, so as to win the Hund's exchange energy with the $d_{1\uparrow}$ electron (at the expense of some loss of the bonding energy). This would stabilize the MO (or rather $\widetilde{MO}$) state ever more, shifting the critical value J^c_H needed for stabilizing DE state to larger values (i.e., $J^c_H \sim 6t_c$, and not $J^c_H \sim 2t_c$ as follows from Eq. **3**). That is, the electron hopping can be even more efficient in suppressing DE than it follows from the simple estimate in Eq. **5**.

Model Consideration

In fact such a model with two orbitals per site and three electrons per dimer can be solved exactly (see the details in *Supporting Information*; here and below we used the Hubbard model within the Kanamori parameterization rather than a simplified expression for the interaction term given in Eq. **2**), including also the onsite Coulomb (Hubbard) repulsion *U*, besides the Hund's rule exchange J_H and the hopping of *d* and *c* orbitals (t_c and t_d). The corresponding phase diagram for $T=0$ K is shown in Fig. 3.

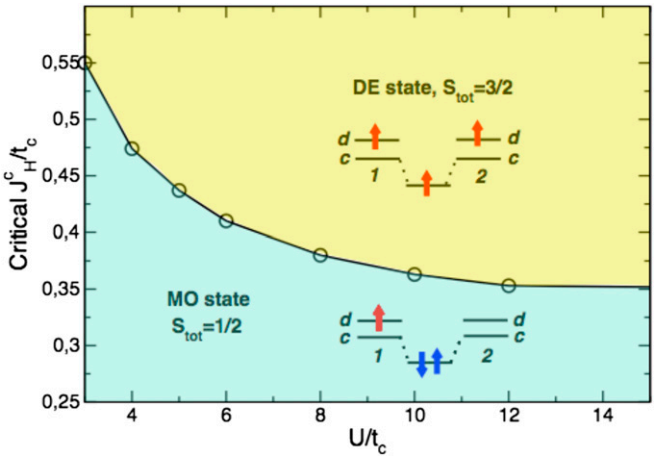

Fig. 3. Phase diagram for a dimer with two orbitals (c and d) per site and three electrons in U (onsite Hubbard repulsion) and J_H (Hund's rule coupling) coordinates; c orbitals form molecular orbitals (corresponding hopping is t_c), and d orbitals stay localized ($t_d = 0.1t_c$, the same as in Fig. 4). Results of the exact diagonalization at $T = 0$ K. We restrict ourselves only by the repulsive Coulomb potential, which in the Kanamori parameterization corresponds to $U > 3J_H$.

One may see that indeed the MO state can be realized for any U, if J_H is small enough. This state can be considered as orbital selective (23), because only d orbitals provide local moments, and electrons on c orbitals form spin singlet. For a finite U the simple estimates such as Eq. **5** do not hold anymore, and the critical value J_H^c needed to stabilize the DE state is much smaller than for $U = 0$, because the Coulomb repulsion modifies the ground-state wave function for c electrons from real molecular orbital to the Heitler–London, or rather Coulson–Fisher-like, with an increased weight of the ionic terms (with respect to homopolar ones) (24). The transition from one state to another is discontinues, since they are characterized by different quantum numbers ($S_{tot} = 3/2$ for DE state vs. $S_{tot} = 1/2$ for MO state), and corresponding terms do not hybridize, but simply cross.

We can generalize this treatment onto larger systems, which we did for a dimerized chain with 2 orbitals and 1.5 electrons per site. The calculations have been performed using a cluster version of the dynamical mean-field theory (DMFT) (25). The cluster DMFT was shown to provide a very accurate description of the one-dimensional chain (25). The results of the cluster DMFT calculations for a dimerized chain at a fixed U are shown in Fig. 4. We see that indeed the MO-like state with $S_{tot} = 1/2$ survives for realistic values of J_H (for 4*d*–5*d* materials) (20, 21) and the DE can be suppressed for small J_H even in an extended system. The transition to this MO state is not discontinuous now, but is broadened, because of two factors: temperature (which is one of the parameter in our cluster-DMFT calculations) and formation of bands, or in other words the presence of the finite electron hoppings between dimers. As it was explained above, the critical Hund's rule coupling strongly depends on U. If U is small, then J_H competes with the difference of hopping parameters, $t_c - t_d$, which defines the energy of the MO. In contrast, with increasing U we quickly arrive at the Heitler–London type of the wave function for c electrons with the energy gain $\sim t_c^2/U$ in the MO state.

Role of the Spin–Orbit Coupling

As the effects discussed in this paper are met mainly in 4*d* and 5*d* compounds (although not exclusively, see the discussion about CrO_2), it is important to address the possible role of spin–orbit coupling (SOC), which is strong in these systems. It turns out that the effect of SOC is not universal and depends on a specific situation.

Consider first the same situation with three electrons per dimer and threefold degenerate t_{2g} orbitals, which now can be labeled by value of z projection of the effective orbital moment $l = 1$, i.e., $|l^z = 0\rangle \equiv |0\rangle$ and $|l^z = \pm 1\rangle \equiv |\pm 1\rangle$. For the sake of simplicity here and below we consider SOC on the one-electron level, i.e., $H_{SOC} = -\sum_m \zeta \vec{l}_m \vec{s}_m$ (here m numerates orbitals). Then for weak SOC, $\zeta \ll (t_c, J_H)$, we can again have two situations: that of the DE, with the maximum spin for a dimer possible, here $S_{tot} = 3/2$, Fig. 5*A*, and the state with the singlet MO and the total spin $S_{tot} = 1/2$, Fig. 5*B*. To gain at least some SO energy, we put localized electrons with spin $\uparrow$ on the orbital $|+1\rangle$. Because in the most geometries such as edge and face sharing the orbitals with $l_z = 0$ (xy and a_{1g} orbitals, respectively) strongly overlap, we put itinerant electrons on the bonding orbital $\frac{1}{\sqrt{2}}(|0\rangle_1 + |0\rangle_2)$, where 1 and 2 are site indexes. The energy of the DE state in this case is

$$E^{DE}_{weak-SOC} = -t_c - J_H - \zeta, \qquad [7]$$

(cf. Eq. **1**), because here for localized electrons only the "classical" part of the SOC contributes in lowest order, $-\zeta\langle 1,\uparrow|l^z s^z|1,\uparrow\rangle = -\zeta/2$ per site, and in the lowest order the bonding states with $l_z = 0$ do not give energy gain due to SOC (it will appear due to "quantum" terms $l^+ s^-$, etc., in the second order in ζ/t_c). Similarly, the energy of the MO state of Fig. 5*B* is

$$E^{MO}_{weak-SOC} = -2t_c - J_H/2 - \zeta/2, \qquad [8]$$

(cf. Eq. **4**). Comparison of these expressions shows that in this case SOC stabilizes magnetic DE state: the condition for low-spin MO state is now, instead of Eq. **5**,

$$2t_c > J_H + \zeta. \qquad [9]$$

This agrees with results of ref. 26, where the case of the weak SOC was considered.

However, the situation is very different for strong SOC, $\zeta \gg (t_c, J_H)$. In this case we can project relevant states onto a quartet $j = \frac{3}{2}$, with the states $|j^z = \frac{3}{2}\rangle = |1,\uparrow\rangle$, $|j^z = \frac{1}{2}\rangle = \sqrt{\frac{2}{3}}|0,\uparrow\rangle + \sqrt{\frac{1}{3}}|1,\downarrow\rangle$, $|j^z = -\frac{1}{2}\rangle = \sqrt{\frac{2}{3}}|0,\downarrow\rangle + \sqrt{\frac{1}{3}}|-1,\uparrow\rangle$, $|j^z = -\frac{3}{2}\rangle = |-1,\downarrow\rangle$. Then the "DE" state with the maximum total moment j of a dimer 7/2 is the state shown in Fig. 5*C*, with localized d electrons on sites 1 and 2 in states $|j^z = 3/2\rangle$, and a "mobile" electron—on a bonding orbital

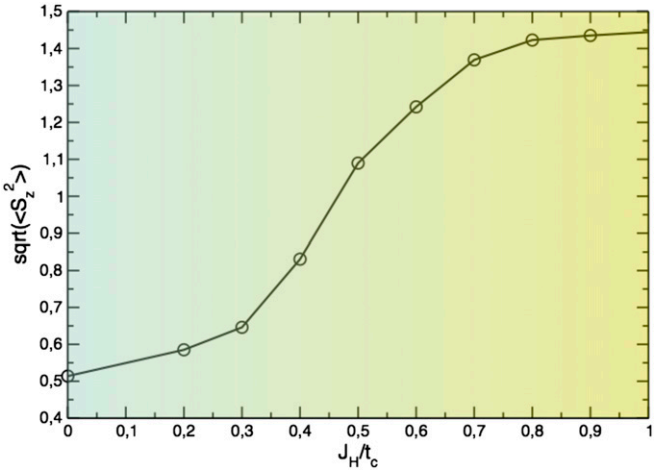

Fig. 4. Dependence of $\sqrt{\langle S^2_{tot,z}\rangle}$ on the J_H/t_c ratio at fixed $U = 6t_c$ for a dimerized chain with 1.5 electrons and with 2 orbitals per site at $T = 1{,}100$ K. Intradimer hopping parameter for d orbitals was taken to be $0.1t_c$, and interdimer hopping $t_c' = t_d' = 0.05t_c$; Results of the cluster DMFT calculations.

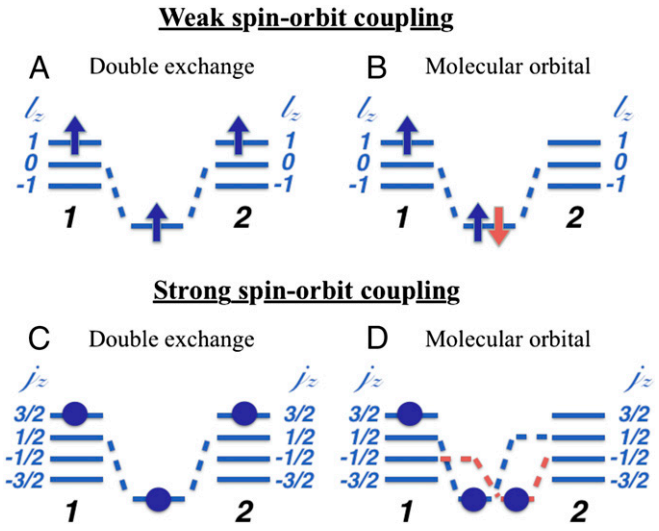

Fig. 5. Two competing electronic configurations for a dimer—DE and MO in the case of weak (*A* and *B*) and strong (*C* and *D*) spin–orbit coupling, three t_{2g} orbitals per site and three electrons.

$\frac{1}{\sqrt{2}}(|j^z{=}1/2\rangle_1 + |j^z{=}1/2\rangle_2)$. For such state the effective hopping is reduced, as only the $|0\rangle$ component "hops" to a neighbor, $\langle j^z = \pm\frac{1}{2}|\hat{t}|j^z = \pm\frac{1}{2}\rangle = \frac{2}{3}\langle 0|\hat{t}|0\rangle = \frac{2}{3}t_c$, and the total energy of such state turns out to be

$$E^{DE}_{strong-SOC} = -\frac{2}{3}t_c - \frac{3}{2}\zeta - \frac{2}{3}J_H \qquad [10]$$

(SOC energy in any state of the quartet $j=\frac{3}{2}$ is $-\zeta/2$ per electron; the calculation of the Hund's energy contribution is quite straightforward, but somewhat tedious). We treat the Hund's energy in a mean-field approximation, using the "recipe" described for example in ref. 2: the Hund's energy is equal to $J_H \times$(number of parallel spins, see Eq. S1). More accurate treatment of the Hund's coupling, including quantum effects in it, would somewhat change numerical coefficients, but would not change qualitative conclusions. In our numerical and ab initio calculations presented below the Hund's rule coupling is taken into account in a more rigorous way, including quantum effects in it.

Similarly, an analog of the MO state is shown in Fig. 5*D*. In this state we put one electron on a localized state $|j^z=\frac{3}{2}\rangle$, say on a site 1, and two electrons on bonding orbitals $\frac{1}{\sqrt{2}}(|j^z{=}\frac{1}{2}\rangle_1 + |j^z{=}\frac{1}{2}\rangle_2)$ and $\frac{1}{\sqrt{2}}(|j^z{=}{-}\frac{1}{2}\rangle_1 + |j^z{=}{-}\frac{1}{2}\rangle_2)$. The energy of this state, calculated similarly to that of the DE state in this regime, is

$$E^{MO}_{strong-SOC} = -\frac{4}{3}t_c - \frac{3}{2}\zeta - \frac{13}{18}J_H. \qquad [11]$$

We see that in this regime (strong SOC) the MO state is definitely favored over the DE state: the contribution from the SOC in any state of a quartet is the same, and in the MO state both the bonding and even Hund's energies are lower.

Summing up, in the case of three electrons per dimer weak SOC acts in favor of the magnetic DE state, but strong SOC, instead, stabilizes the MO state with reduced moment. This is related to the fact that the energy of the bonding orbital (the lowest curve in Fig. S1) rapidly decreases with the increase of SOC, which makes the MO state (in which this orbital is occupied twice) more favorable.

The analytic treatment presented above is confirmed by the exact diagonalization results for the dimer with three orbitals per site. The resulting phase diagram is shown in Fig. 6. We see that it agrees with our analytical results for limiting cases of $\zeta \to 0$ and $\zeta \to \infty$ presented above, and it has a "reentrant" character: for certain values of parameters the increase of SOC can initially transform system into the magnetic DE state, but for larger ζ - back to the MO state.

One may expect that for the weak SOC the situation is similar also not for three electrons, but for three holes in t_{2g} levels [situation typical, for example, for a dimer of, formally, $Ir^{4+}(d^5)$ and Ir^{5+} (d^4)]. However, for strong SOC we do not have anymore the electron–hole symmetry: as is well known (2, 27), these states can be projected onto a Kramers doublet $j=1/2$ without any extra orbital degeneracy, and for the situation with d^4/d^5 occupation (nine electrons per dimer) only the analog of a low-spin state with the total moment 1/2 is possible. Thus, in this case the qualitative phase diagram would again have the form similar to the one shown in Fig. 6, with weak SOC stabilizing magnetic DE state, but strong SOC suppressing total moment—although mathematical description is different from the case with three *d* electrons.

However, for example one can show that the situation is qualitatively different for five electrons per dimer: in this case the treatment similar to that for three electrons above, shows that both strong and weak SOC works in favor of a less-magnetic MO state, i.e., the corresponding curve separating MO and DE states in the phase diagram, similar to that of Fig. 6, would increase already at small ζ, without reentrant behavior. Thus, we see that, in contrast to the Hund's coupling, which always competes with the electron hopping and tends to stabilize a "more magnetic" state, the SOC can work differently in different situations.

One more important factor, which can change the interplay of SOC with the Hund's exchange and electron hopping, is a possible contribution of not only the direct *d*–*d* hopping, considered in our treatment, but also of the hopping via *p* orbitals of ligands, e.g., oxygens. To take into account all these effects, for real materials it is probably better to rely on ab initio calculations, the results of some of which are presented in the next section.

Suppression of the Double Exchange and Magnetic Moment in Real Materials

We now turn to real materials and show that the physics described above (strong reduction of magnetic moment and eventual suppression of double exchange, due to formation of orbital-selective covalent bonds between TM) indeed works in real materials and allows us to explain the behavior of many 4*d* and 5*d* systems. The first example of such a system is the recently synthesized oxyfluoride $Nb_2O_2F_3$ (28) (see its structure in Fig. S2 and the results of our ab initio calculations in *Supporting Information*). Although, according to the chemical formula there

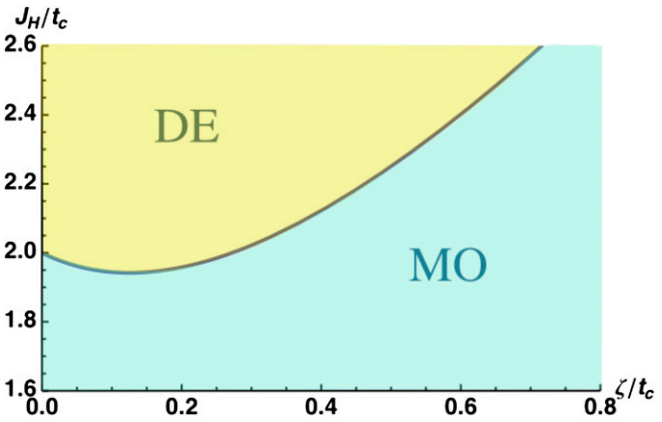

Fig. 6. Phase diagram for a dimer with three t_{2g} orbitals per site and three electrons, which takes into account spin–orbit coupling on the one-electron level. Results of the exact diagonalization at $T=0$ K.

has to be three d electrons per Nb dimer, i.e., $S_{tot} = 3/2$, the experimental effective magnetic moment is consistent with $S_{tot} = 1/2$ per dimer (28). The band-structure calculations show that the bonding–antibonding splitting for the xy orbitals pointing to each other in the common edge geometry (cf. Fig. 1*A*) is very large here, $2t_c \sim 4$ eV—much larger than the Hund's rule energy estimated to be $J_H \sim 0.5$ eV for Nb (21).

According to the results of our model cluster DMFT calculations, see above, for $J_H/t_c \sim 0.25$ the DE is largely suppressed, which agrees with the experimental findings (28). However, parameters t_d, t', U in $Nb_2O_2F_3$ can be very different from what we used in the model calculations, so that comparison with the results (see Fig. S3) of the generalized gradient approximation (GGA) should be more appropriate. These results are summed up in *Supporting Information*, and indeed show that the value of the local magnetic moment in the high temperature phase is $\mu^{theor} \sim 1\mu_B$ per dimer, which agrees with the experimental value of the effective moment (28, 29).

We have discussed so far how covalent bonding competes with Hund's rule coupling. However, as discussed above, for 4*d* and 5*d* TM compounds also another "player" can enter the game: the spin-orbit coupling, which is known to be strong enough in heavy 4*d*/5*d* metals and has been already demonstrated to cause very unusual physical effects (30–32). On our second example, $Ba_5AlIr_2O_{11}$, we show that this interaction may indeed take part in the competition between intra-atomic exchange and covalent bonding.

The crystal structure of $Ba_5AlIr_2O_{11}$ consists of $[Ir\text{-}Ir]^{9+}$ dimers (Fig. S4*A*) with nine electrons or three holes per dimer, so that this is exactly the example of a system, considered in the first part of our paper, where the DE and MO states could compete. Indeed, the effective magnetic moment in the Curie–Weiss law $\mu_{eff} \sim 1\mu_B$/dimer, measured at high temperatures, indicates substantial suppression of the magnetic moment (33). However, our GGA calculations show that accounting for covalency and exchange splitting is not sufficient to explain this small μ_{eff}; they give $\mu^{GGA} \sim 2\mu_B$. It is the spin–orbit coupling, that, by additional splitting of d levels, conspires with the covalency and finally helps to suppress the DE in this system, see *Supporting Information*. However, as stressed in the previous section, this is not a general conclusion: depending on the filling of the d shell and on a specific geometry, the spin–orbit interaction can act against the DE or support it.

Until now we have considered real materials in which the structure provides relatively well-separated dimers. As we saw, e.g., in our cluster DMFT calculations, the effect of suppression of the DE can survive even for solids, without well-defined dimers. In some of such systems singlet covalent bonds can form spontaneously, also acting against DE (cf. ref. 34).

One such example seems to be given by CrO_2—a classical DE system (35). In CrO_2 one of the two 3*d* electrons is localized in the xy orbital on each Cr site, and another one occupies a broad xz/yz band, stays itinerant and actually makes this system ferromagnetic (35). In contrast to VO_2, having the same rutile structure, but one d electron per V, CrO_2 does not dimerize at zero pressure.

Apparently, in normal conditions in this system the hopping via oxygens is more important, and in effect DE wins and provides ferromagnetism with large Curie temperature. However, under high pressure the situation can change: the direct *d*–*d* hopping can begin to dominate, the bonding–antibonding splitting even in this 3D system can become comparable with what we have in 4*d* and 5*d* TM compounds at normal conditions, in which case our physics could come into play. Indeed, accurate band-structure calculations (36) have found a cascade of structural transitions in CrO_2 with pressure, with the formation of the dimerized monoclinic structure for $P \sim 70$ GPa. As in the case of the Jahn–Teller distortions, it is not clear whether the lattice or electronic subsystem triggers the structural transition, but once the dimerization starts they go hand in hand and destabilize the DE state by lowering the energy of the xy molecular orbital. At some point two out of four d electrons in the Cr–Cr dimer occupy this molecular orbital, and the remaining two electrons provide metallicity and eventual paramagnetism, similar to what is observed in MoO_2 at normal conditions (37) or expected in $MoCl_4$ at moderate pressure (38). We thus see that even some 3*d* systems could in principle be tuned to the MO regime, in particular under pressure, which increases *d*–*d* overlap and hopping, making such systems more similar to the 4*d* and 5*d* ones.

It is also possible that some other factors, such as charge ordering (29), could modify the situation. The external perturbations, such as temperature or pressure, can drive a system from the DE to the MO state, so that the phase diagrams of systems with competing DE and MO states can be rather rich and their physical properties can be highly unusual.

Conclusions

In conclusion, we demonstrated in this paper that the standard approach to describe the magnetism in solids with strongly correlated electrons, proceeding from the isolated ions in their ground state, and adding electron hopping between ions perturbatively, may break down in certain situations, especially for 4*d* and 5*d* systems. In particular, due to large *d*–*d* hopping orbital-selective covalent bonds, or singlet molecular orbitals between transition metal ions may form in this case. This would lead to a strong suppression of the effective magnetic moment, and, for fractional occupation of d shells, can strongly reduce or completely suppress the well-known double exchange mechanism of ferromagnetism. Several examples of real material considered in our paper indeed demonstrate that this mechanism is very efficient in suppressing the double exchange in a number of 4*d* and 5*d* compounds, and can even operate in some 3*d* systems. Spin–orbit coupling, especially relevant for 4*d* and 5*d* compounds, can also play an important role and in many cases it works together with electron hopping to suppress magnetic state, although in some situations it can also act in opposite direction. Our results show yet one more nontrivial effect in the rich physics of systems with orbital degree of freedom, especially those close to Mott transition.

ACKNOWLEDGMENTS. This work was supported by the Russian Foundation of Basic Research via Grant 16-32-60070, Civil Research and Development Foundation via Program FSCX-14-61025-0, FASO (theme "Electron" 01201463326), Russian Ministry of Education and Science via act 11 Contract 02.A03.21.0006, by Köln University via the German Excellence Initiative, and by the Deutsche Forschungsgemeinschaft through SFB 1238.

1. Imada M, Fujimori A, Tokura Y (1998) Metal-insulator transitions. *Rev Mod Phys* 70(4): 1039–1263.
2. Khomskii DI (2014) *Transition Metal Compounds* (Cambridge Univ Press, Cambridge, UK).
3. Sachdev S (2001) *Quantum Phase Transitions* (Cambridge Univ Press, New York).
4. Anderson PW (1959) New approach to the theory of superexchange interactions. *Phys Rev* 115:2.
5. Zener C (1951) Interaction between the d-shells in the transition metals. II. Ferromagnetic compounds of manganese with perovskite structure. *Phys Rev* 82:403.
6. Plumb KW, et al. (2014) Alpha-RuCl3: A spin-orbit assisted Mott insulator on a honeycomb lattice. *Phys Rev B* 90(4):41112.
7. Sears JA, et al. (2015) Magnetic order in alpha-RuCl3: A honeycomb-lattice quantum magnet with strong spin-orbit coupling. *Phys Rev B* 91(14):144420.
8. Kimber SAJ, et al. (2014) Valence bond liquid phase in the honeycomb lattice material Li$_2$RuO$_3$. *Phys Rev B* 89:081408.
9. Wang JC, et al. (2014) Lattice-tuned magnetism of Ru4+(4d4) ions in single crystals of the layered honeycomb ruthenates Li2RuO3 and Na2RuO3. *Phys Rev B* 90(16):161110.
10. Sheckelton JP, Neilson JR, Soltan DG, McQueen TM (2012) Possible valence-bond condensation in the frustrated cluster magnet LiZn2Mo3O8. *Nat Mater* 11(6): 493–496.
11. Mourigal M, et al. (2014) Molecular quantum magnetism in LiZn2Mo3O8. *Phys Rev Lett* 112(2):027202.
12. Chaloupka J, Jackeli G, Khaliullin G (2010) Kitaev-Heisenberg model on a honeycomb lattice: Possible exotic phases in iridium oxides A2IrO3. *Phys Rev Lett* 105(2):027204.
13. Choi SK, et al. (2012) Spin waves and revised crystal structure of honeycomb iridate Na2IrO3. *Phys Rev Lett* 108(12):127204.

14. Foyevtsova K, Jeschke HO, Mazin II, Khomskii DI, Valent R (2013) Ab initio analysis of the tight-binding parameters and magnetic interactions in Na2IrO3. *Phys Rev B* 88: 035107.
15. Goodenough JB (1963) *Magnetism and the Chemical Bond* (Interscience Publishers, New York).
16. Kugel KI, Khomskii DI, Sboychakov AO, Streltsov SV (2015) Spin-orbital interaction for face-sharing octahedra: Realization of a highly symmetric SU(4) model. *Phys Rev B* 91(15):155125.
17. Khomskii DI, Kugel KI, Sboychakov AO, Streltsov SV (2016) Role of local geometry in the spin and orbital structure of transition metal compounds. *J Exp Theor Phys* 122(3): 484–498.
18. de Gennes PG (1960) Effects of double exchange in magnetic crystals. *Phys Rev* 118: 141.
19. Anderson PW, Hasegawa H (1955) Considerations on double exchange. *Phys Rev* 100(2):675.
20. Sawatzky GA, van der Marel D (1988) Electron-electron interaction and localization in d and f transition metals. *Phys Rev B Condens Matter* 37(18):10674–10684.
21. Sasioglu E, Friedrich C, Blugel S (2011) Effective Coulomb interaction in transition metals from constrained random-phase approximation. *Phys Rev B* 83(12):121101.
22. Streltsov SV (2015) Orbital-selective behavior in Y5Mo2O12 and (Cd,Zn)V2O4. *J Magn Magn Mater* 383:27.
23. Streltsov SV, Khomskii DI (2014) Orbital-dependent singlet dimers and orbital-selective Peierls transitions in transition-metal compounds. *Phys Rev B* 89:161112.
24. Coulson CA, Fischer I (1949) XXXIV. Notes on the molecular orbital treatment of the hydrogen molecule. *Philos Mag* 40(December):386.
25. Kotliar G, Savrasov SY, Pálsson G, Biroli G (2001) Cellular dynamical mean field approach to strongly correlated systems. *Phys Rev Lett* 87:186401.
26. Isobe H, Nagaosa N (2014) Generalized Hund's rule for two-atom systems. *Phys Rev B* 90:115122.
27. Abragam A, Bleaney B (1970) *Electron Paramagnetic Resonance of Transition Ions* (Clarendon Press, Oxford, UK).
28. Tran TT, et al. (2015) Nb2O2F3: A reduced niobium (III/IV) oxyfluoride with a complex structural, magnetic, and electronic phase transition. *J Am Chem Soc* 137(2):636–639.
29. Gapontsev VV, Khomskii DI, Streltsov SV (2016) Magnetism and charge ordering in high- and low-temperature phases of Nb2O2F3. *J Magn Magn Mater* 420:28–32.
30. Kim BJ, et al. (2008) Novel Jeff=1/2 Mott state induced by relativistic spin-orbit coupling in Sr2IrO4. *Phys Rev Lett* 101(7):076402.
31. Jackeli G, Khaliullin G (2009) Mott insulators in the strong spin-orbit coupling limit: From Heisenberg to a quantum compass and Kitaev models. *Phys Rev Lett* 102(1): 017205.
32. Witczak-Krempa W, Chen G, Kim YB, Balents L (2014) Correlated quantum phenomena in the strong spin-orbit regime. *Annu Rev Condens Matter Phys* 5(1):57–82.
33. Terzic J, et al. (2015) Coexisting charge and magnetic orders in the dimer-chain iridate Ba5AlIr2O11. *Phys Rev B* 91:235147.
34. Nishimoto S, Ohta Y (2012) Double exchange ferromagnetism in the Peierls insulator state. *Phys Rev Lett* 109(7):076401.
35. Korotin M, Anisimov V, Khomskii D, Sawatzky G (1998) CrO$_2$: A self-doped double exchange ferromagnet. *Phys Rev Lett* 80(19):4305.
36. Kim S, Kim K, Kang CJ, Min BI (2012) Pressure-induced phonon softenings and the structural and magnetic transitions in CrO_{2}. *Phys Rev B* 85(9):094106.
37. Eyert V, Horny R, Höck K, Horn S (2000) Embedded Peierls instability and the electronic structure of MoO$_2$. *J Phys Condens Matter* 12:4923.
38. Korotin DM, Anisimov VI, Streltsov SV (2016) Pressure-induced magnetic transitions with change of the orbital configuration in dimerised systems. *Sci Rep* 6(April):25831.
39. Momma K, Izumi F (2011) VESTA 3 for three-dimensional visualization of crystal, volumetric and morphology data. *J Appl Cryst* 44:1272.
40. Hirsch JE, Fye RM (1986) Monte Carlo method for magnetic impurities in metals. *Phys Rev Lett* 56(23):2521–2524.
41. Perdew JP, Burke K, Ernzerhof M (1996) Generalized gradient approximation made simple. *Phys Rev Lett* 77(18):3865–3868.
42. Blaha P, Schwarz K, Madsen G, Kvasnicka D, Luitz J (2001) *WIEN2k, An Augmented Plane Wave + Local Orbitals Program for Calculating Crystal Properties* (University of Wien, Wien).